ELSEVIER

FEMS Microbiology Ecology 30 (1999) 171–186

FEMS MICROBIOLOGY ECOLOGY

# Comparison of *Nitrosospira* strains isolated from terrestrial environments

Qing Qiao Jiang [a], Lars R. Bakken [b,*]

[a] *Department of Biotechnological Sciences, Agricultural University of Norway, 1432 Aas, Norway*
[b] *Department of Soil and Water Sciences, Agricultural University of Norway, 1432 Aas, Norway*

Received 23 September 1998; revised 22 June 1999; accepted 22 June 1999

**Abstract**

Most of our knowledge about the physiology of ammonia-oxidizing bacteria is based on experiments with *Nitrosomonas europaea*, which appears to be less ubiquitous than *Nitrosospira*. We have isolated *Nitrosospira*s from widely different environments and compared their specific growth rate, substrate affinity, urease activity, temperature response, pH tolerance and cell morphology. Two of the strains had a variable morphology: the spirals were less tightly coiled than the classical *Nitrosospira* type and a fraction of the culture had a vibrioid appearance. These vibrioid strains were also peculiar in having a much higher apparent activation energy for ammonia monooxygenase (AMO) (129 and 151 kJ $mol^{-1}$) than that of the more classical *Nitrosospira*s (78 and 79 kJ $mol^{-1}$). The differences in morphology and activation energy were congruent with the phylogeny of the genes for 16S rRNA (Utåker et al., System. Appl. Microbiol. 18) and AMO. The response to pH in the medium was investigated for four strains. The oxidation rate at the onset of the pH exposure experiment was found to obey classical steady state enzyme kinetics, assuming that $NH_3$ (not $NH_4^+$) is the rate-limiting substrate. The calculated half saturation constants ($K_s$) for AMO were 6–11 μM $NH_3$. Growth had a narrower pH range than oxidation activity and appeared to be restricted by pH-dependent factors other than $NH_3$. All the isolated strains were urease positive, with a specific urease activity ranging from 60 to 158% of their specific AMO activity. The urease activity was unaffected by acetylene inhibition of the energy metabolism. The substrate affinity for one strain was found to be around 670 μM. 

*Keywords:* Ammonia-oxidizing bacterium; Ecophysiology; Nitrification; Urease; Soil; *Nitrosospira*

## 1. Introduction

The oxidation of ammonia to nitrate (nitrification) in soil is primarily attributed to autotrophic bacteria, of which ammonia-oxidizing bacteria (AOB) carry out the first step, i.e. the oxidation of ammonia to nitrite. AOB is thus a crucial functional group and their ecophysiology is a determinant factor for the N-dynamics in soil. Compared to other functional groups in soil, AOBs have a low diversity, slow growth rate, sensitivity to acidity and a to whole range of chemicals [1]. Autotrophic nitrifiers are typically diminished through successions in terrestrial ecosystems. Soils under the climax type of plant

* Corresponding author. Tel.: +47 (6494) 8219; Fax: +47 (6494) 8211; E-mail: lars.bakken@ijvf.nlh.no

0168-6496/99/$20.00 
PII: S0168-6496(99)00054-9

communities are typically harboring lower numbers of autotrophic nitrifiers than more juvenile stages [2–4]. The early taxonomy of AOB was entirely based on cell morphology and five different genera were recognized, i.e. *Nitrosococcus, Nitrosospira, Nitrosolobus, Nitrosovibrio* and *Nitrosomonas* [5]. Based on the 16S rRNA gene sequences [6–9], a reclassification of AOB has been suggested, placing the three morphological types *Nitrosospira*, *Nitrosovibrio*, and *Nitrosolobus* within one common genus (*Nitrosospira*) and retaining *Nitrosomonas* and *Nitrosococcus* as separate genera [8]. The relative importance of the different AOBs in soil is difficult to judge, due to the inherent bias of the culturing techniques. Based on the relative frequency of isolation, MacDonald [10] tentatively concludes that *Nitrosolobus* is the most important genus. Judging from the frequency of isolation of cells with a *Nitrosospira* morphology over the last couple of decades [11–15], this genus seems to be at least as ubiquitous as those with a *Nitrosolobus* morphology. Despite the apparently minor ecological role of *Nitrosomonas europaea*, practically everything that is known about the physiology of AOBs is based on experiments with this bacterium. This warrants a comparative study of some basic characteristics of the apparently more ubiquitous *Nitrosospira*s.

In the present study, *Nitrosospira*s previously isolated from different environments by extinction dilution were compared with respect to specific metabolic activity (ammonium oxidation and urea hydrolysis) and growth rate in response to the temperature, substrate concentrations and acidity.

## 2. Materials and methods

### 2.1. Cultures

The cultures were isolated from widely different environments. Strain AF: cultivated red sandy soil (pH 4.0) from Kasama, Zambia [16]; strain L115: ombrotrophic peat (pH 4.0) from the Lakkasuo area in Finland [17]; strain B6: pebbles (pH 6.3) from the nitrifying reactor in a sewage treatment plant (VEAS, Oslo, Norway); strain 40K1: cultivated clay loam soil (pH 6.5) from Aas, Norway [18]; III2 and III7: acid forest soils (pH 3.9 and 4.1, respectively) near the Agricultural University in Aas, Norway.

The phylogenetic positions of the strains have been determined by their 16S rDNA sequences [8,9]. L115 and AF were placed in one cluster (*Nitrosospira* type I). The other *Nitrosospira*s (B6, 40Kl, III2 and III7) were placed in another cluster (*Nitrosospira* type II). The phylogeny of ammonium monooxygenase (AMO) genes of some strains (40K1, L115, III2 and III7) was congruent with the phylogeny based on the 16S rDNA sequences (Utåker, unpublished).

### 2.2. Isolation and cultivation

The strains were isolated by extinction dilution as described previously [8]. The basic medium was a liquid mineral (LM) medium [19] supplemented with a trace element solution [20]. The LM medium contained (per l of MilliQ water) $KH_2PO_4$, 0.2 g; $CaCl_2 \cdot 2H_2O$, 0.02 g; $MgSO_4 \cdot 7H_2O$, 0.04 g; Fe-NaEDTA, 3.8 mg; phenol red, 0.1 mg; $NaMoO_4 \cdot 2H_2O$, 0.1 mg; $MnCl_2$, 0.2 mg; $CoCl_2 \cdot 6H_2O$, 0.002 mg; $ZnSO_4 \cdot 7H_2O$, 0.1 mg and $CuSO_4 \cdot 5H_2O$, 0.02 mg. When used for isolation, sodium carbonate was added to regulate the pH and ensure the supply of $CO_2$. When used for culturing and physiological experiments, the medium was supplemented with HEPES buffer (2-(4-2-hydroxyethyl-1-piperazinyl)-ethanesulfonic acid sodium salt, Merck, 15231). Unless otherwise stated, the HEPES concentration was 15 mM. When the cultures were secluded from access to atmospheric $CO_2$ (i.e. in sealed serum bottles), 0.84 mM $Na_2CO_3$ was added to ensure sufficient $CO_2$ for growth. When supplied with ammonium as the energy substrate ($(NH_4)_2SO_4$), the medium is denoted LMA, when supplied with urea, the medium is denoted LMU. Unless otherwise stated, the concentrations of ammonium sulfate and urea were 3.8 mM. Cultivation was always conducted in the dark.

### 2.3. Electron microscopy examinations

Cells for electron microscopy observations were grown in 500-ml Erlenmeyer flasks containing 150 ml of LMA medium, which were incubated on a rotary shaker at 22°C. The pH was regulated fre-

quently (to pH = 7–7.5) by adding a 6% solution of $Na_2CO_3$. At the late exponential phase (cell density around $10^7$ cells $ml^{-1}$), the cells were harvested by centrifugation (Sorvall RC-5B Refrigerated Superspeed Centrifuge, Du Pont Instrument) at $10\,000 \times g$ for 15 min. The cells were fixed in glutaric dialdehyde (2.5%, final concentration in LMA medium), rinsed in 50 mM (pH = 7) cacodylate buffer ($3 \times 15$ min), post-fixed (2 h) in 2% $OsO_4$ (same buffer) and rinsed again (same buffer) before dehydration through an ethanol gradient (70–100%), propylene oxide and finally embedded in Spurr epoxy resin [21]. Ultra-thin transversal sections (80 nm) of the epoxy-embedded cells were stained with uranyl acetate [22] and lead citrate [23] and viewed in a JEOL 1200EX microscope (80 kV). For negative staining, cells were adsorbed to a carbon-coated copper grid (400 mesh), rinsed with water, stained with uranyl acetate, rinsed again and viewed with the same microscope as the thin sections. For scanning electron microscopy (SEM), cells were first adsorbed onto cover glass surfaces pretreated with polylysine (mw 70–150 000, Sigma), dehydrated through an ethanol gradient and critical point-dried using $CO_2$ as the transitional fluid. The cover glasses were then mounted with colloidal silver on aluminum stubs and coated with platina/palladium in a sputter coater before examination in a JEOL 850 microscope (15 kV).

### 2.4. Physiological experiments

#### 2.4.1. Inoculum preparation

Cells for physiological experiments were grown in the LMA medium buffered with 20 mM HEPES. The initial pH of the medium was adjusted to pH 7.5. A volume of 300 ml was inoculated with 1 ml culture stock solution and incubated at 22°C on a shaker (100 rpm). To ensure a homogenous culture with few dead cells, it was considered important to use cells from an actively growing culture (before depletion of the ammonium). This was checked by measuring the nitrite level during culturing. The cells were harvested when approximately 2/3 of the ammonium was oxidized. Harvesting was done by filtration on 25-mm Nuclepore polycarbonate filters with a 0.2-μm pore size (Costar Europe, Badhoevedorp, The Netherlands). To harvest cells from 300 ml culture, 3–4 filters had to be used due to clogging of filters. The cells collected on the filters were washed off by shaking in 20 ml LM medium. After removing the filters, cell dispersion was ensured by pumping 15–20 times through a 0.5-mm hypodermic needle on a 20-ml syringe. The suspension was then kept at 22°C on a shaker and used as an inoculum within 3 h after preparation. Cell density in the inoculum was determined by fluorescence microscopical counts of cells retained on polycarbonate membranes after staining with acridine orange [24].

#### 2.4.2. Specific activity, growth rate and growth yield

The cultures were grown in 250-ml Erlenmeyer flasks containing 60 ml LMA medium buffered with 50 mM HEPES, pH regulated to 7.8. The flasks were inoculated with 0.6 ml cell suspension, resulting in an initial cell density of $2–7 \times 10^5$ cells $ml^{-1}$. The incubation was carried out at 22°C on a reciprocal shaker (100 rpm). The incubation time was 120 h and samples ($2 \times 1$ ml) were taken at 6, 24, 48 and 120 h for nitrite determination and cell counts. Initial cell numbers were counted and the samples for cell counts (fluorescence microscopy) were preserved by adding glutaric dialdehyde to a final concentration of 2.5%. The experiment was duplicated.

#### 2.4.3. Effect of temperature

A series of 100-ml Erlenmeyer flasks was filled with 25 ml LMA medium buffered with 50 mM HEPES, pH regulated to pH 7.5, and placed in thermostated incubators at 3, 9, 15, 21, 26, 31, 36 and 41°C. The flasks were left in the incubators overnight prior to inoculation, to ensure temperature equilibration. The flasks were then inoculated with 0.2 ml of the prepared inoculum (final cell density $2–7 \times 10^5$ cells $ml^{-1}$). Samples (1 ml) for nitrite determination were taken after 6 and 12 h. The samples were snap-frozen in an ethanol bath (−18°C) and kept frozen until analysis. The experiment was duplicated.

#### 2.4.4. Effect of pH

A series of liquid LMA media with pH levels ranging from 5 to 8.5 were prepared. The media contained 50 mM HEPES and the pH in each batch was adjusted by adding 1 N HCl or NaOH. Erlenmeyer flasks (250 ml) were filled with 60 ml medium (two replicate flasks for each pH level). The flasks

were then inoculated with 0.6 ml of the inoculum, resulting in an initial cell density of $2–7\times10^5$ cells $ml^{-1}$. The incubation was carried out at 22°C on a reciprocal shaker (100 rpm). Sampling was done as described for the temperature experiment.

*2.4.5. Urease activity and growth on urea*

Duplicate 250-ml Erlenmeyer flasks containing 60 ml LMU medium (1 mM urea) were inoculated to a cell density of $10^5–10^6$ cells $ml^{-1}$ and incubated at 22°C on a reciprocal shaker (100 rpm). Control flasks were included which were 'inoculated' with cell-free suspensions prepared exactly the same way as the inocula, in order to reveal any trace of urease activity that could stem from other sources than the cells. As a second control, flasks were inoculated with a *N. europaea* known to be urease negative. Samples (3 ml) were taken at intervals during the 240-h incubation, to determine nitrite and ammonium (i.e. $NH_3+NH_4^+$) and cell numbers. Each culture was run in duplicate.

One of the cultures, L115, was investigated further with respect to the urease activity and its dependency on substrates and the energy status of the cells. Cells for inoculum were grown in LMA medium (1 mM $(NH_4)_2SO_4$). The cells were harvested and used to inoculate 40-ml batches of LMU medium (0.3 mM urea), contained in 120-ml serum bottles capped with Teflon-faced silicone/PTFE septa (20-ST3, Chromacol, London, UK). The initial cell density was $1.5\times10^6$ cells $ml^{-1}$. Two bottles were supplied with acetylene ($C_2H_2$) to a final concentration of 1% (v/v) in the gas phase, to inhibit AMO. The bottles were incubated at 22°C on a reciprocal shaker (100 rpm) for 3 days. Samples (1 ml) for determination of ammonium and nitrite were taken with a 0.5-mm needle through the septa. In a follow up experiment, a near complete depletion of urea was obtained by using a higher cell density (approximately $10^7$ $ml^{-1}$) in an otherwise identical experiment, in order to use the urea depletion curve in the acetylene-inhibited culture to assess the substrate affinity of the urease.

L115 was also used to check for the presence of extracellular urease activity. The cells were grown in 100 ml LMU medium (1 mM urea) buffered with 5 mM HEPES (pH = 7.8). When 1/2–2/3 of the substrate was oxidized, the pH of the culture was adjusted to 7 and the cells were removed by centrifugation ($7000\times g$ for 40 min) in a HS34 swing out rotor, using a Sorval RC5B centrifuge. Urease activity was then measured in the original culture and the cell-free culture fluid by incubating in the presence of urea (0.3 mM urea added) under a 1% (v/v) acetylene atmosphere (in sealed serum flasks) to inhibit AMO. At intervals during a 100-h incubation at 22°C, samples were taken with a syringe to determine ammonium ($NH_3+NH_4^+$) and urea.

*2.4.6. Data analysis, estimation of kinetic parameters*

The ammonia oxidation rate in the temperature experiments was calculated using the data of nitrite formation between 6 and 12 h of incubation. For the other experiments, the data for nitrite accumulation for longer periods of incubation were used to estimate the kinetic parameters, using a function described by Stenstrom et al. [25]. It is assumed that the rate of product ($NO_2^-$) formation ($dp/dt$) is proportional to the number of cells, $N$, $dp/dt = qN$, where $q$ is the specific production rate per cell unit. Assuming exponential growth of $N$ ($N = N_0*\exp(\mu t)$), the integrated product accumulation is

$$p = p_0 + (q * N_0/\mu)(\exp(\mu * t)-1) \quad (1)$$

where $p_0$ is the product concentration at $t = 0$, $N_0$ is the number of active cell units at $t = 0$, $\mu$ is the specific growth rate ($h^{-1}$) and $t$ is the incubation time (h). The values for $\mu$ and the product $qN_0$ were estimated by non-linear regression of this function (Eq. 1) against measured nitrite accumulation, using the Simplex routine in version 5.2 of the SYSTAT computer program (SYSTAT, Evanston, IL, USA). The value of $p_0$ was zero in our case, due to removal of nitrite by the filter harvesting of cells for inoculation. The estimated value for $q*N_0$ is of particular interest in the pH experiment, since it estimates metabolic activity in response to pH at time zero, i.e. before any growth or decline of the metabolic activity has taken place.

The growth rate ($\mu$) and the initial number of active cells ($N_0$) were also estimated through non-linear regression based on the microscopically determined cell numbers, assuming a regular exponential growth function:

$$N = N_0 * \exp(\mu * t) \quad (2)$$

By combining the $N_0$ estimate based on Eq. 2 and

the estimates for $\mu$ and the product $qN_0$ based on Eq. 1, we calculated the specific metabolic activity per cell, $q$, and the growth yield, $Y$ (cells per mol of substrate oxidized).

The square root model of Ratkowsky et al. [26] was used to describe the temperature response over the entire temperature range. The model describes the reaction rate (or growth rate) as follows: $k^{1/2} = b(T - T_{min})(1 - \exp(c^*(T - T_{max})))$, where $b$ and $c$ are 'shape parameters' and $T_{max}$ and $T_{min}$ are the maximal and minimal temperatures (not necessarily equal to the absolute limits, though). The function was fitted to the empirical data by non-linear regression (SYSTAT). This curve fitting exercise was performed only to enhance the graphical presentation of the data. The measured metabolic activities in the lower temperature range (3–21°C) were used to determine the apparent activation energy of the rate-limiting reaction, by linear regression of ln ($V$) against $T^{-1}$, where $V$ = measured oxidation rate and $T$ = temperature (K).

The estimated activity at time zero in the pH experiment (i.e. the product $qN_0$, estimated by regression using Eq. 1 as outlined above) was expected to be a Michaelis-Menten function of the concentration of $NH_3$, which again is a function of the pH. This was inspected by calculating the $NH_3$ concentration for each pH level and plotting the inverse value of the $qN_0$ against the inverse value of the calculated $NH_3$ concentration (Burk-Lineweaver plot). Since fairly straight lines were obtained, the half saturation constants ($K_s$) were estimated by linear regression.

#### 2.4.7. Cell counts and chemical analyses

Cell numbers were determined by fluorescence microscopical counts [24]. To ensure complete dispersion of the cells prior to staining and filtration, the samples were dispersed by pumping through a syringe needle, stained with acridine orange and mounted on polycarbonate filters [24]. In experiments where growth was estimated by cell counts, two filters for microscopy were prepared for each culture flask (at each sampling). Nitrite was determined by using Griess-IIosvay reagents I and II with a flow injection system (FIA star, Tecator AB, Sweden). Ammonium was also determined with the FIA system (Application Sub Note ASN 151-01/92, Tecator AB, Sweden). Urea was analyzed by the diacetyl monoxime method [27].

## 3. Results

### 3.1. Electron microscopy examination

All strains were Gram-negative spiralled cells (Fig. 1) with a variable number of coils per unit. Strain AF had a much larger cell diameter (around 0.5 μm) than the five others (0.2 μm). Strain B6 and 40Kl (Fig. 1A) always remained tightly coiled, whereas the two 'vibrioid' types (AF and L115) demonstrated a morphological variability ranging from vibrioid rods (Fig. 2B) to more normally spiralled types (Fig. 2A) although the coiling was less tight than for B6 and 40Kl. Strain L115 was even more morphologically variable than strain AF (Fig. 2C and D). The morphology of the other strains (III2 and III7) was very similar to 40K1.

### 3.2. Specific activity and growth rate, effects of pH

Table 1 summarizes the specific activities per cell, growth yields and generation times estimated from

Table 1
Specific activities per cell, growth yields and generation times, based on the measured nitrite accumulation and cell counts (acridine orange direct counts (AODC))

| Strain | Activity ($q$) (fmol $NO_2^-$ cell$^{-1}$ h$^{-1}$) | Yield ($Y$) (cells pmol$^{-1}$) | Generation time ($T_d$)[a] (hours) | |
|---|---|---|---|---|
| | | | $NO_2^-$ | AODC |
| B6 | 4.3 | 2.8 | 58 | 50 |
| 40Kl | 6.0 | 1.8 | 63 | 58 |
| L115 | 5.3 | 2.7 | 50 | 63 |
| AF | 7.1 | 0.7 | 139 | 138 |

[a]Based on non-linear regression of nitrite accumulation data ($NO_2^-$) and cell counts by AODC.

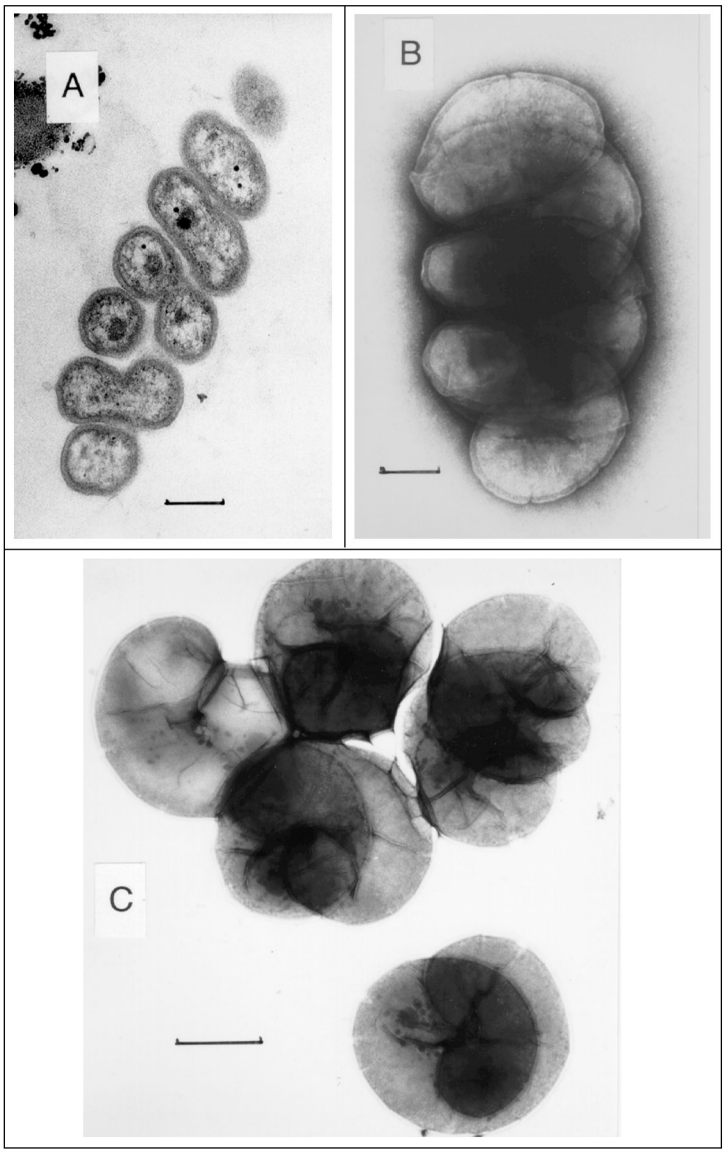


Fig. 1. The spiralled morphology of the isolated ammonia-oxidizing bacteria, illustrated by a thin section through a tightly coiled cell of strain 40Kl (A), a negatively stained cell coil of strain L115 (B) and shorter spirals of the strain AF (C). Bar = 0.2 μm (A and B), 0.5 μm (C).

the first comparative growth experiment. The generation times calculated from product formation agreed reasonably well with those calculated from microscopical counts. The three strains B6, 40Kl and L115 had similar generation times, contrasting AF which had an extremely slow growth rate.

Fig. 3 shows the nitrite accumulation in the pH experiment for strain 40Kl. Since oxidation of ammonia to nitrite will acidify the medium, the pH was measured in all the samples in order to check if the activity significantly changed the pH of the medium. No measurable changes occurred, however (data not shown), attributable to the fact that the molar concentration of HEPES buffer (50 mM) was more than

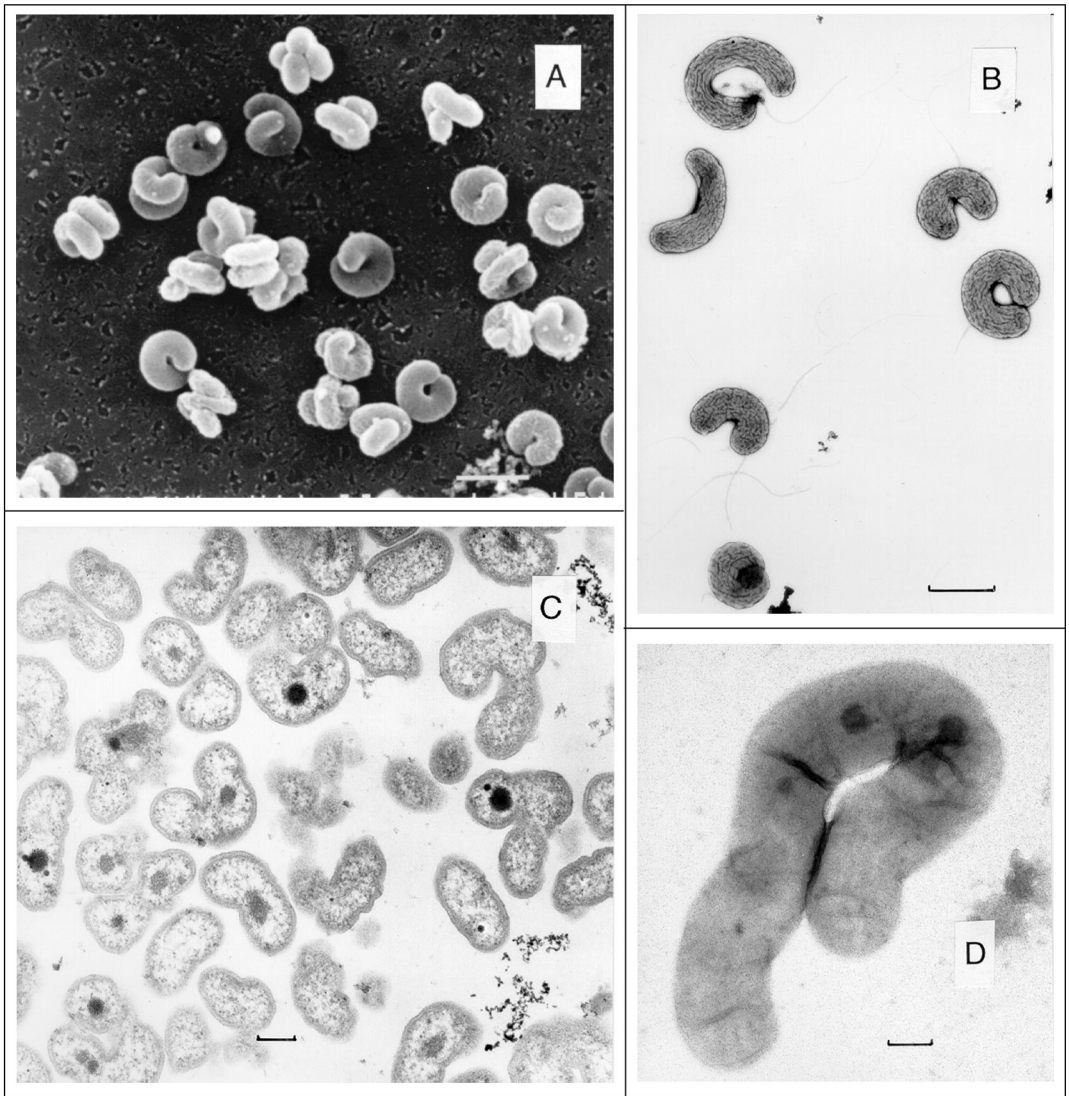


Fig. 2. Morphological variability of the 'vibrioid' *Nitrosospira* strains, illustrated by negatively stained cells of strain AF recently after isolation (B), SEM picture of the strain after some transfers in the laboratory (A), thin sections of L115 (C) and a negatively stained cell of strain L115 (D). Bar = 1 μm (A and B), 0.2 μm (C and D).

50 times higher than the net $H^+$ production through oxidation of ammonia to nitrite.

The rate of nitrite production (Fig. 3) increased with time at optimal pH levels, reflecting growth under such conditions. In contrast, the rate of nitrite formation was practically constant at pH 6. At pH 8.5, a substantial decline in the nitrite formation rate can be seen, indicating a gradual inhibition or lethal effects of the high pH values. Thus, the nitrite formation data contain information about two different phenomena: the specific activity per cell in response to the pH ( = the initial rate of nitrite formation) and the growth (or death) of the cells in response to pH. To separate these phenomena, the nitrite formation data were used to estimate the growth (or death) rate and the activity at time zero (i.e. $\mu$ and $qN_0$, see Section 2) by non-linear regression. The non-linear regression was done for each single flask (two repli-

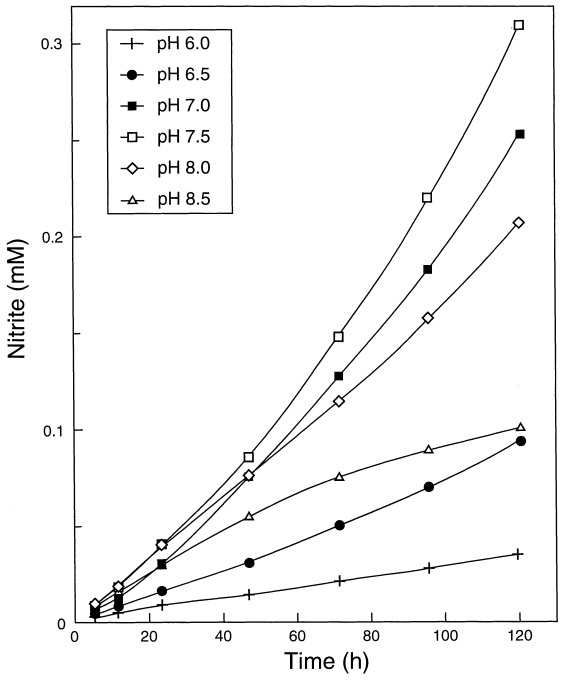


Fig. 3. Nitrite accumulation as a function of pH in the medium, strain 40Kl.

cates for each pH level) and the results are presented in Fig. 4, as relative values (% of maximal values for each culture). Straight lines between average values at each pH level are included to enhance the readability of the figure.

The result for 40Kl shows that metabolic activity at time zero ($qN_0$) occurs over a rather wide pH range (5.5–8.5), whereas growth seems to be restricted to a pH range from 6.5 to 8.0. Outside this range, the rate of nitrite formation declined with time (Fig. 3), resulting in negative estimates of $\mu$ (Fig. 4). Negative $\mu$ values at pH 8.5 were also found for AF and B6.

In general, the cultures were similar with respect to their relative metabolic activity ($qN_o$) in response to the pH, although they had different lower limits for detectable activity (the only culture with detectable nitrite production at pH 5.0 was AF). In contrast, the estimated growth rates ($\mu$, Fig. 4) revealed more profound differences between the cultures. Strain 40Kl had an exceptionally narrow pH range for growth compared to that of the others. Strain L115 represents an extreme in being able to grow at pH 8.5.

The curves for the metabolic activity at time zero ($qN_0$) were expected to be a function of the $NH_3$ concentration, since $NH_3$ is the substrate for AMO (rather than $NH_4^+$). This was inspected by calculating the $NH_3$ concentration for each pH value and plotting the inverse value of $qN_0$ against the inverse value of the $NH_3$ concentration (i.e. Burk-Lineweaver). There was a remarkably good linear relationship between the inverse values, clearly demonstrated by Fig. 5 and by the high correlation coefficients (Table 2). The estimated half saturation constants ($K_s$) based on the regressions of the inverse values gave similar results for the different strains (Table 2).

### 3.3. Specific activity and growth rate, temperature response

During the short (12 h) incubation time, less than 50 μM ammonium was oxidized to nitrite. Thus, the oxygen consumed by the culture was an order of magnitude lower than the initial oxygen concentration of the medium (which is around 1 mM for distilled water at 30°C when in equilibrium with the atmosphere). Thus, oxygen limitation is unlikely to have occurred. The temperature response and the square root function fitted by non-linear regression for each culture is shown in Fig. 6. The African strain (AF) had a much higher activity than the others at high temperatures (20–35°C) and lower values than the others at the lower temperature range. The temperature response in the lower temperature range was used to estimate the apparent activation

Table 2
Half saturation substrate constants ($K_s$) and apparent activation energies ($E_a$)

| Strain | $K_s$ (μM $NH_3$)[a] | | $E_a$ (kJ $mol^{-1}$)[b] | |
|---|---|---|---|---|
| | $K_s$ | $r^2$ | $E_a$ | $r^2$ |
| 40Kl | 11 | 0.988 | 77 | 0.964 |
| AF | 6 | 0.977 | 149 | 0.989 |
| B6 | 8 | 0.995 | 75 | 0.974 |
| L115 | 9 | 0.970 | 129 | 0.933 |

[a] $K_s$ estimated by linear regression of inverse values of the activity at time zero ($qN_0$) and concentrations of ammonia, as illustrated in Fig. 5.
[b] $E_a$ estimated by linear regression of the natural logarithm of activity against the inverse of the absolute temperature (K), as illustrated in Fig. 7.

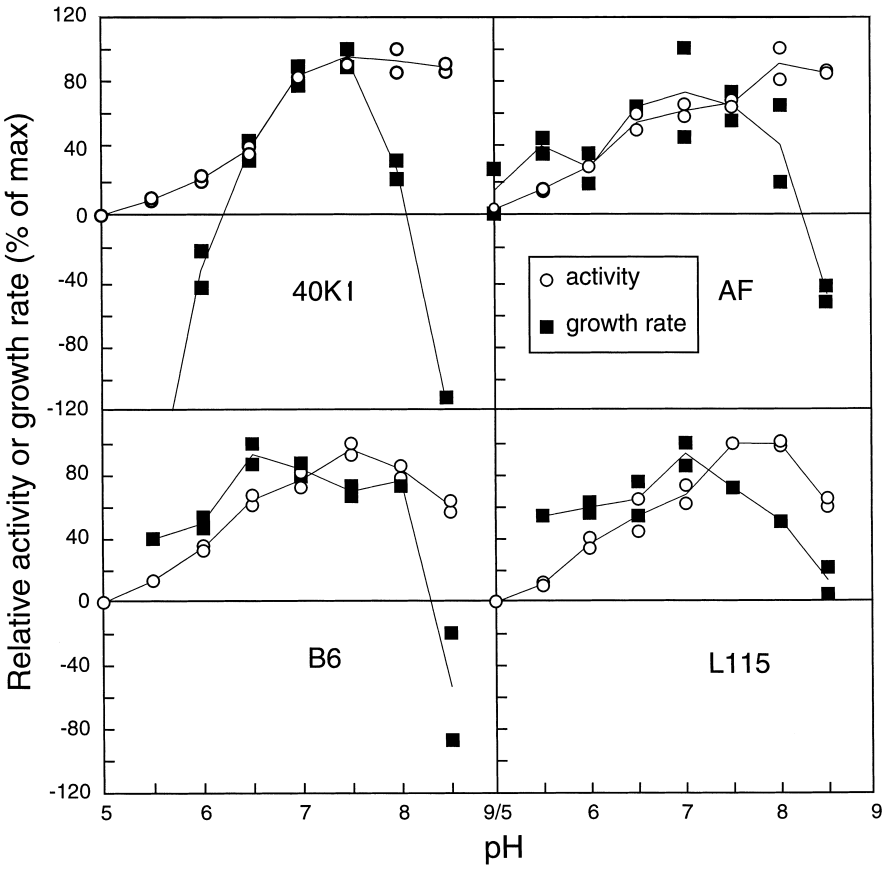


Fig. 4. Relative values for the estimated growth rate constant ('growth rate') and ammonia oxidation rate at the onset of the incubation ('activity') in response to the pH in the medium. Single flask estimates are presented as % of maximum values for each strain, straight lines are drawn between average values. Both variables are based on non-linear statistical analysis of the nitrite accumulation curves (see text for further explanation). The scaling of the axis precluded a presentation of negative growth rates for 40Kl at pH 5.5 (−167 and −200%).

energy of the rate-limiting enzyme reaction. Plotting of the exponential values of the oxidation rate (ln ($V$)) against the inverse of the absolute temperature ($T^{-1}$, $K^{-1}$) revealed a reasonably linear relationship, but only for temperatures up to 21°C. This is illustrated in Fig. 7, where single flask values of ln ($V$) are plotted together with the linear regression functions for each strain. The correlation coefficients and the estimated apparent activation energy of the rate-limiting enzyme reaction based on these data are shown in Table 2. The correlation coefficient for L115 was lower than the others, due to a deviation from the linear relationship at 21°C (i.e. the points on the left extreme of Fig. 7). If this point is excluded, the correlation coefficient is higher (0.949) and the estimated activation energy, $E_a$, is 159 kJ $mol^{-1}$.

### 3.4. Urease activity

All the tested *Nitrosospira* strains grew well on urea, resulting in a transient accumulation of ammonium in the medium. In the control flasks without cells, a low and constant level (0.1 mM) of ammonium was found, possibly due to an initial hydrolysis of urea during autoclaving. In the flasks inoculated with *N. europaea*, this low initial amount of ammonium was gradually oxidized (recovered as nitrite), but no further oxidation nor cell proliferation was detected (data not shown).

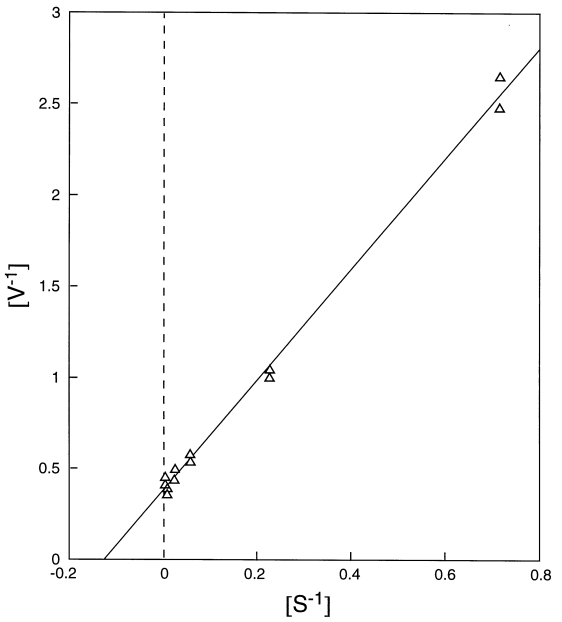


Fig. 5. Plot of inverse values of the ammonia oxidation rate by strain B6 ($V^{-1}$) against inverse values of the $NH_3$ concentration ($S^{-1}$). The points are values for each separate flask, used to estimate the $K_s$ by regression (Table 2).

Approximate estimates of the urease and ammonia oxidation activity per cell during the early phase of the experiment (less than 50% of the urea hydrolyzed) were calculated as the net increase in the products (ammonium+nitrite) divided by the average cell count for each time increment (mean value of cell counts at the beginning and at the end of the time increment). The result for 40K1 is shown in Fig. 8, where the ratio between the two enzyme activities is plotted as well. The activities per cell increased with time, whereas the ratio between them was practically constant. The other cultures showed similar patterns in having increasing specific enzyme activities per cell prior to depletion of the substrates and a fairly constant ratio between the two enzyme activities through the same period of the experiment. The average urease/AMO ratios were 0.6, 0.85, 0.96, 1.24, 1.31 and 1.58 (unit: mol urea $h^{-1}$ $mol^{-1}$ ammonia $h^{-1}$) for L115, B6, III7, III2, AF and 40K1, respectively.

Acetylene (1%) inhibited ammonium oxidation and growth of L115, but urease activity was unaffected and practically constant through a 3-days incubation (result not shown). In the second experiment with a higher cell density, the curvature of the urea depletion in the presence of acetylene (Fig. 9) was used to estimate the substrate affinity of the urease enzyme, by regression using the linearized form of the integrated Henri-Michaelis-Menten equation [28], which gave a $K_m$ of 670 μM. The smooth curve illustrates the simulated (simple Euler) urea concentration ($S$) assuming that $dS/dt = V_{max}*S/(S+K_m)$, with $V_{max} = 19$ μM $h^{-1}$ and $K_m = 670$ μM (which were found by linear regression).

## 4. Discussion

### 4.1. Is the isolation frequency of Nitrosospiras reflecting their importance in soil?

The protocol for isolation, using the extinction dilution as the first step, ensures that the isolates obtained will be dominated by species that occur in

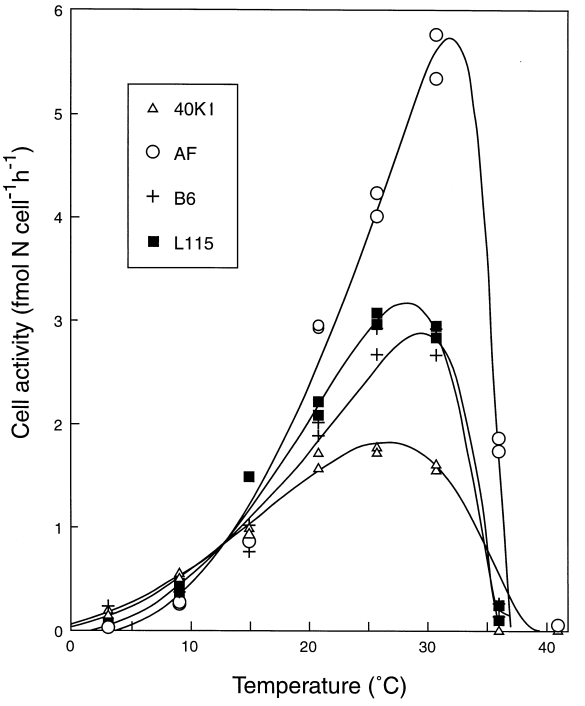


Fig. 6. Rate of ammonia oxidation (6–12-h incubation increment) as a function of the temperature, presented as single flask values and the fitted 'square root model' [25].

relatively high numbers among the culturable cells in soil. Culturability is an operational criterion, however, defined by the medium and growth conditions. The tendency of *Nitrosomona* species to form cell clusters which are difficult to disperse [29] is possibly a bias against this group. The low rate of success when purifying newly isolated strains of AOB is yet another source of bias. What if some cultures are more easy to purify than others? There are two obvious reasons for such a selectivity in the purification procedure. Firstly, surface properties which result in strong adhesion to surfaces and heterotrophic organisms will make purification extremely difficult, hence the purification selects against such properties. Secondly, there will be a selection against large cells, since such organisms will produce a lower number of cells per mol of $NH_3$ oxidized (i.e. they are more likely to be outnumbered by the heterotrophic organisms, hence not successfully isolated).

On this background, the successful isolation of

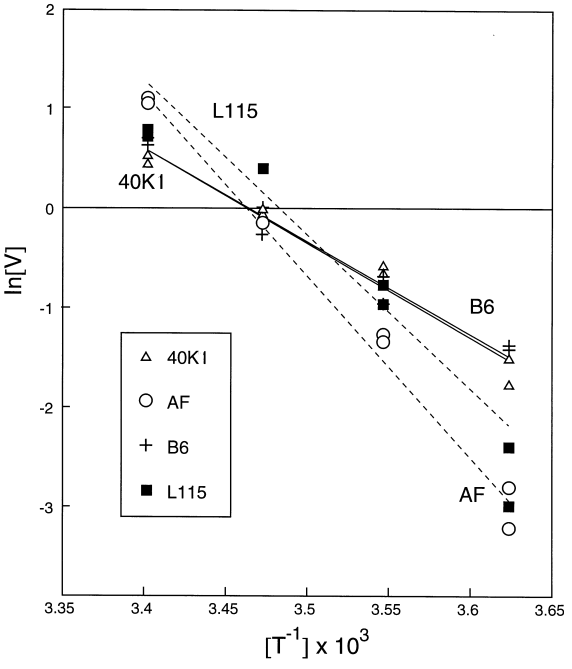


Fig. 7. Analysis of apparent activation energy for the rate-limiting reaction. The natural logarithm of the ammonia oxidation rate (ln ($V$)) plotted against the inverse of the temperature ($T^{-1}$, $K^{-1}$), single flask values and linear regression lines for each culture (dotted lines: L115 and AF). The correlation coefficients and the estimated apparent activation energy (based on the slope of the regression line) are shown in Table 2.

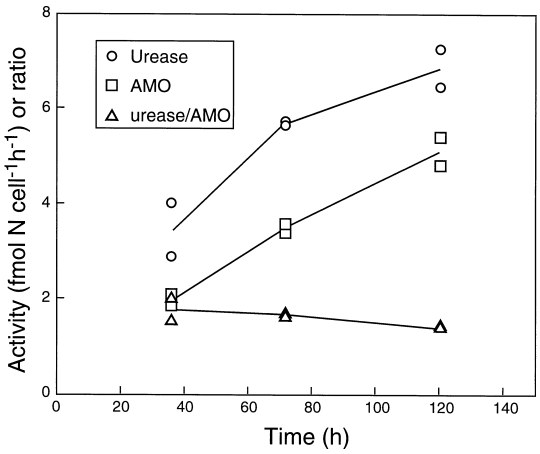


Fig. 8. Calculated specific rates of urea hydrolysis ('urease') and ammonia oxidation ('AMO') and the ratio between the two reaction rates ('urease/AMO') during the early phase of growth of 40K1 on urea. Single flask values for each of the first three time increments (24–48 h, 48–96 h and 96–144 h) are shown, straight lines are drawn between average values for each time increment.

*Nitrosospira*s in this study does not prove that this type is dominating in the environments they were isolated from, but it seems reasonable to conclude that the numbers of *Nitrosospira*s in these environments are not negligible compared to other culturable ammonia-oxidizing species. On the other hand, the predominance of *Nitrosomonas* in enrichment cultures from soils, determined by selective PCR on DNA extract from such enrichments [30], proves the ubiquity of this group of ammonia oxidizers as well. The predominance of *Nitrosomonas* in enrichment cultures is probably attributable to their relatively rapid growth compared to *Nitrosospira*s.

*Nitrosospira* has often been isolated from acid soils [11–14,31] and for this reason, it has been suggested that a low pH selects for *Nitrosospira*. Urease activity is one trait that could support growth of *Nitrosospira*s under acid conditions [14]. Extreme acid tolerance (pH = 4) of a specific strain of *Nitrosospira* [32] is another observation that supports the notion that a low pH selects for *Nitrosospira*s. However, *Nitrosospira*s are apparently not confined to acid conditions, as judged from their isolation from more alkaline environments such as lake sediments [33,34]. The ubiquity of *Nitrosospira*s in other environments than acid soils has also been demonstrated by analyzing total DNA extract from lake water

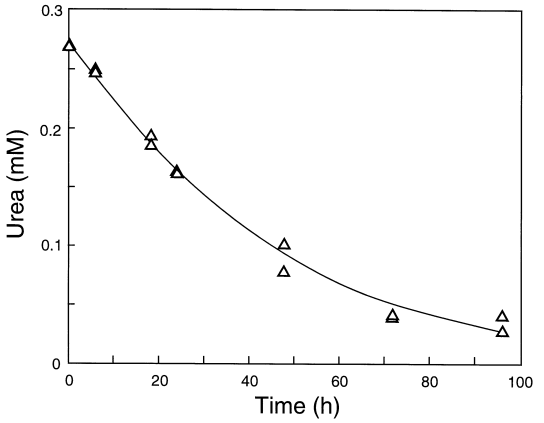


Fig. 9. Depletion of urea in a heavily inoculated suspension of L115 in the presence of acetylene (to inhibit growth and de novo enzyme synthesis). The curve shows the predicted depletion curve, assuming Michaelis-Menten kinetics and a $K_m$ value of 670 μM (estimated by regression).

samples and sediments, using PCR with primers that are specific for the *Nitrosospira* and *Nitrosomonas* group [35]. Our isolation of *Nitrosospira*s both from acid (AF and L115) and neutral (40Kl and B6) environments is yet another indication that this genus is a very ubiquitous AOB.

### 4.2. Are the vibrioid cultures pure?

The peculiar variable/vibrioid morphology of L115 and AF is congruent with the clustering based on 16S rDNA sequencing [8,9], which placed these strains in a group containing strains previously belonging to *Nitrosovibrio*. The change in morphology which was observed in AF and L115 could be suspected to be due to the presence of two genotypes. However, this does not seem likely, since there was a complete homology of the 16S rDNA sequences before and after the morphological change (Utåker, unpublished). The purity has later been confirmed by analyzing their RFLP patterns [36].

### 4.3. Activity as a function of pH: a function of the $NH_3$ concentration

The fact that nitrification commonly occurs in soil with pH values far below the limits for laboratory grown pure cultures has inspired to search for 'acidophilic nitrifiers' [13]. Urease positive *Nitrosospira*s have been isolated from acid soils [37] and if urea is present, this might contribute to their acid tolerance [38]. Further, a strain of *Nitrosospira* was shown to be able to remain active even at pH levels down to 4.0, if allowed to adapt gradually during growth [32]. None of the cultures in the present study proved to be particularly acid tolerant, although AF was able to maintain a low activity and growth at pH 5. The discrimination between the specific ammonia oxidation rate per cell (at the onset of the pH exposure) and growth revealed that the specific oxidation rate responded similarly for all the cultures and could largely be described by the steady state enzyme kinetic response to substrate concentrations (i.e. $NH_3$). The calculated half saturation constants ($K_s$ = 6–11 μM $NH_3$) were considerably lower than the range of values (18–58 μM) calculated by Suzuki et al. [39] for *N. europaea*. Knowles et al. [40] measured $K_s$ values for mixed cultures of indigenous estuarine nitrifying bacteria at different temperatures. They estimated the $K_s$ to be around 70 μM $NH_3$ for experiments around room temperature. Stehr et al. [41] based their calculated substrate affinities for *Nitrosomonas* species on the sum of $NH_4^+$ and $NH_3$ in a medium of pH = 7.8 and found extremely high values for *N. europaea* isolated from brackish water (420 μM). However, if estimated for $NH_3$ (which is only around 3.5% of the total $NH_4^+ + NH_3$ at pH = 7.8), the $K_s$ is only 12 μM $NH_3$, which is comparable to the values for our *Nitrosospira*s.

### 4.4. Growth as a function of pH is a more complex matter

In contrast to the oxidation rate at time zero, for which there were only minor differences between the cultures, the calculated growth rate as a function of pH revealed profound strain differences. Strain 40Kl was particularly sensitive to low pH values, whereas AF represents the other extreme in tolerating pH values down to 5. The acid tolerance reflects the pH value of the environment from which the strains were isolated: 40Kl was isolated from neutral (limed) clay loam soil, whereas AF and L115 were isolated from acid soils. This suggests that acid soils exert a selection pressure favoring acid tolerance among the ammonia oxidizers. The evolved acid tolerance (in

AF and L115) is not due to an improved ability to capture substrate ($NH_3$) at low pH values, however, as judged from the similarity in half saturation constants (Table 2). Similarly, the lack of acid tolerance for 40Kl is hardly due to a poor ability to capture substrate ($NH_3$) at a low pH. The increased acid tolerance of AF and L115 seems to involve an improved tolerance to $H^+$ concentrations as such or to the pH-dependent toxicity of nitrite, although the nitrite concentrations were practically zero at the start of the pH experiment due to the filter harvesting of the cells for inoculum.

The negative effect of the moderately high pH values contrasts with *N. europaea*, which is able to grow at pH values at least as high as 8.5–9.0 [39]. The sensitivity to pH values of 8.5 has practical consequences for the maintenance of cultures, if buffered by adding carbonate solutions during cultivation. A slight over-shoot in pH easily occurs and if this exceeds 8.0–8.5, three of the four tested strains (40Kl, AF and B6) would probably die. Loss of cultures has been encountered from time to time in our lab (Ågot Aakra, Janne Utåker, Lars Bakken, Qing Qiao Jiang, personal confessions) and one possible reason may be too high pH values in the medium.

### 4.5. Temperature models

The calculated activities per cell in the temperature experiment (Fig. 6) were much lower than those calculated in the growth experiment (Table 1). One reason for this might be an overestimation of the number of active cells in the temperature experiment, since the calculated activity per cell for this experiment was based on a total microscopical count of the inoculum. If the inoculum contains inactive cells, the calculated specific activity will be underestimated accordingly. Such errors are less important in the growth experiment due to growth of active cells (hence active cells will outnumber the inactive ones after a few generations). Another factor might be that the cultures were incubated stationary in the temperature experiment, whereas the other experiments were conducted with shaking.

The square root model by Ratkowsky et al. [26] proved to give a fairly adequate representation of the response over the entire temperature range for each organism. The simplicity of the model and its adequacy in describing the response over the entire temperature range has been one rationale for using this model [42–44]. The graphical presentation of the data and the model (Fig. 6) give a strong impression of a major difference between the African strain (AF) and the three others with respect to the optimal temperature (31–33 versus 26–29°C, respectively) as well as to the activity at low temperatures (AF lower than the others). The difference between the African strain and the Nordic ones probably reflects a selective pressure by the climate, favoring higher optimum and maximum temperatures in tropical areas. This has also been demonstrated by analyzing the temperature response of whole nitrifying communities of soils from different climatic regions [45]. The optimum temperatures of the strains from the Nordic soils (40Kl and L115) are similar to that for another *Nitrosospira* strain isolated from Finish forest soil [15].

The disadvantage of the square root model is that the parameters do not have any mechanistic meaning (hence not reported here). A more analytical approach was to plot the exponential values of the activities against the inverse of the absolute temperature, which would yield a straight line provided that the reaction rate (ammonia oxidation to nitrite) is limited by a single enzyme reaction (and that the conformation of this key enzyme is unaltered by the temperature). Fairly linear relationships were obtained for the temperature range 3–21°C, as shown in Fig. 7 (and demonstrated more quantitatively by the high correlation coefficients in Table 2). The calculated apparent activation energies ($E_a$) are surprisingly high and major differences between the strains were revealed. The two strains designated to the 'vibrioid' group based on morphology (Figs. 1 and 2) and the 16S rDNA sequences [8] had very high apparent activation energies ($E_a = 129$ and 149 kJ $mol^{-1}$) compared to the two other strains ($E_a = 78$ and 79 kJ $mol^{-1}$). There is evidently a difference between the two pairs of strains, which could either be due to a difference in a common rate-limiting enzyme or due to the fact that different enzymes are rate-limiting in AF and L115 versus 40Kl and B6.

Our $E_a$ values are high compared to those estimated by the temperature response of growth of *Nitrosomonas* [46] and indigenous assemblages of es-

tuarine nitrifiers [40]. Knowles et al. [40] did not calculate $E_a$ values, but reported the response as exponential functions of temperature. Approximate calculations based on their data yield $E_a$ values around 30 kJ $mol^{-1}$. Painter [46] reports several highly variable experimental results with *Nitrosomonas* which appear to be in some agreement with the responses found by Knowles et al. [40]. One should be aware, however, that the temperature response of growth may be different from that of metabolic activity per cell over short intervals as measured in our temperature experiment, since growth and metabolic activity may not be limited by the same reaction(s).

### 4.6. Congruence between phylogeny and characteristics of the cells

There appears to be some agreement between the morphological and physiological characteristics and the phylogeny of the bacteria. A phylogenetic tree based on the 16S rDNA sequences of the strains in question [8] placed the vibrioid-like strains AF and L115 in a monophyletic group (I) together with *Nitrosovibrio* species and *Nitrosolobus multiformis* and the strains with a more stable spiralled morphology (40Kl, B6, III2 and III7) were placed in another group (II) containing only *Nitrosospira*s. We will use the term *Nitrosospira* type I to denote the vibrioid strains (AF and L115) and *Nitrosospira* type II to denote the strains with the more stable *Nitrosospira* morphology. Common characteristics for the two type I strains (AF and L115) are their high activation energy and their ability to grow at low pH. The activation energy is presumably reflecting properties of the AMO enzyme, since this is the rate-limiting reaction (as demonstrated by the substrate response in the pH experiment). Clustering based on sequencing of a part (525 bp) of the AMO genes (85–98% similarity) was congruent with that based on the 16S rDNA (Utåker, unpublished).

### 4.7. Urease investigations

The transient accumulation of ammonium during growth on urea suggested that urease activity was not directly coupled to oxidation of ammonia. The calculated rates of urea hydrolysis and ammonia oxidation for each time increment (Fig. 8) demonstrated that the ratio between the two process ratios was remarkably constant through the initial part of the growth period (when urea was present in ample amounts). This ratio, which is an approximate estimate of the relative amount of urease activity and ammonia oxidation activity in the active cells, showed clear differences between strains. These differences were not related to the origin of the isolates (acid or neutral soil) or their phylogenetic position (*Nitrosospira* type I versus type II), however.

The calculated rates of urea hydrolysis and ammonia oxidation for the early growth phase of 40Kl (Fig. 8) suggested an increasing activity of both enzymes per cell. This may be due to the presence of inactive cells in the inoculum, but may also reflect an increasing cell size during the incubation. *Nitrosospira*s have a variable number of coils per 'single cell' as counted microscopically and a gradual change from 1 to 2 coils per cell may easily be overlooked during fluorescence counting as done in this experiment.

The subsequent experiment with L115 strongly suggests that urease is constitutive and that the activity is not dependent on the energy status nor the integrity of the cells (thus no active transport is involved). These conclusions are founded on the following observations: acetylene efficiently inhibited the ammonia oxidation, hence prevented any de novo synthesis of enzymes. This inhibition did not affect urease activity, however, which proceeded at a fairly constant rate for 3 days. The lack of detectable urease in the cell-free culture fluid suggests that urease is tightly bound to the cells and/or unable to function outside the cell.

The fact that acetylene inhibited de novo enzyme synthesis but not the activity of the urease was exploited to estimate the half saturation constant ($K_m$) for the urease enzyme in a second experiment. The high inoculum density and the low initial urea concentration ensured a near depletion of the urea, allowing for the half substrate saturation constant ($K_m$) to be estimated by a linearized form of the Michaelis-Menten function. The estimated $K_m$ of 670 μM is in the lower range of $K_m$ values for ureases in other bacteria (ranging from 0.1 to $>100$ mM [47–54]), but it is tremendously high compared to other substrate capturing enzymes in bacteria (normally in the 0.1–1-μM range, [55]). It is also very high compared to ambient bulk concentrations

of urea in soil, which are in the 1–10-μM range (Pedersen H, Ph.D. Thesis 1995, Aarhus University, Denmark). If confronted with such low concentrations, the urease of L115 is of little use, given its $K_m$ of 670 μM. The bulk concentration of urea may be misleading, however, since urea may hypothetically accumulate transiently in hot spots created by the soil fauna (faeces or dead organisms).

## Acknowledgements

We are very grateful to Ms Elisabeth Reed for carrying out many electron microscopy examinations. We thank Dr Tor-Arvid Breland for help in FIA analysis and Dr A. Mapiki for the soil sample from Zambia. The work was financed by the Nordic NKJ project 'Ecological roles of ammonia-oxidizing bacteria in terrestrial environments'.

## References

[1] Bremner, J.M. (1986) Inhibition of nitrogen transformations in soil. In: Proceedings of IV International Symposium on Microbial Ecology (Megusar, F. and Gantar, M., Eds.), pp. 337–342. Ljubljana.

[2] Rice, E.L. and Pancholy, S.K. (1972) Inhibition of nitrification by climax ecosystems. Am. J. Bot. 59, 1033–1040.

[3] Montes, R.A. and Christensen, N.L. (1979) Nitrification and succession in the piedmont of north Carolina. For. Sci. 25, 287–297.

[4] Thorne, J.F. and Hamburg, S.P. (1985) Nitrification potentials of an old-field chronosequence in Campton New-Hampshire USA. Ecology 66, 1333–1338.

[5] Watson, S.W., Bock, E., Harms, H., Koops, H.-P. and Hooper, A.B. (1989) Ammonia-oxidizing bacteria. In: Bergey's Manual of Systematic Bacteriology, Vol. 3 (Staley, J.T., Bryant, M.P., Pfennig, N. and Holt, J.G., Eds.), pp. 1818–1833. Williams and Wilkins, Baltimore, MD.

[6] Head, I.M., Hiorns, W.D., Embley, T.M., McCarthy, A.J. and Saunders, J.R. (1993) The phylogeny of autotrophic ammonia-oxidizing bacteria as determined by analysis of 16S ribosomal RNA gene sequences. J. Gen. Microbiol. 139, 1147–1153.

[7] Teske, A., Alm, E., Regan, J.M., Toze, S., Rittmann, B.E. and Stahl, D.A. (1994) Evolutionary relationship among ammonia- and nitrite-oxidizing bacteria. J. Bacteriol. 176, 6623–6630.

[8] Utåker, J.B., Bakken, L., Jiang, Q.Q. and Nes, I.F. (1995) Phylogenetic analysis of seven new isolates of ammonia-oxidizing bacteria based on 16S rRNA gene sequences. Syst. Appl. Microbiol. 18, 549–559.

[9] Utåker, J.B. and Nes, I.F. (1998) A qualitative evaluation of thepublished oligonucleotides specific for the 16S rRNA gene sequences ofthe ammonia-oxidizing bacteria. Syst. Appl. Microbiol. 21, 72–88.

[10] MacDonald, R.M. (1986) Nitrification in soil: an introductory history. In: Nitrification (Prosser, J.I., Ed.), pp. 1–16. IRL Press, Oxford.

[11] Bhuiya, Z.H. and Walker, N. (1977) Autotrophic nitrifying bacteria in acid tea soils from Bangladesh and Sri Lanka. J. Appl. Bacteriol. 42, 253–257.

[12] Walker, N. and Wickramasinghe, K.N. (1979) Nitrification and autotrophic nitrifying bacteria in acid tea soils. Soil Biol. Biochem. 11, 231–236.

[13] de Boer, W., Duyts, H. and Laanbroek, H.J. (1989) Urea stimulated autotrophic nitrification in suspensions of fertilized, acid heath soil. Soil Biol. Biochem. 21, 349–354.

[14] Allison, S.M. and Prosser, J.I. (1991) Urease activity in neutrophilic autotrophic ammonia-oxidizing bacteria isolated from acid soils. Soil Biol. Biochem. 23, 45–51.

[15] Martikainen, P.J. and Nurmiaho-Lassila, E. (1985) *Nitrosospira*, an important ammonium-oxidizing bacterium in fertilized coniferous forest soil. Can. J. Microbiol. 31, 190–197.

[16] Mapiki, A., Reddy, G.B. and Singh, B.R. (1993) Fate of fertilizer - $^{15}N$ to a maize crop grown in northern Zambia. Acta Agric. Scand. Sect. B Soil Plant Sci. 43, 231–237.

[17] Lien, T., Martikainen, P., Nykänen, H. and Bakken, L.R. (1992) Methane oxidation and methane fluxes in two drained peat soils. Suo 43, 231–236.

[18] Uhlen, G. (1989) Nutrient leaching and surface runoff in field lysimeters on a cultivated soil. Nor. J. Agric. Sci. 3, 33–46.

[19] MacDonald, R.M. and Spokes, J.R. (1980) A selective diagnostic medium for ammonia oxidising bacteria. FEMS Microbiol. Lett. 8, 143–145.

[20] Donaldson, J.M. and Henderson, G.S. (1989) A dilute medium to determine population size of ammonium oxidizers in forest soils. Soil Sci. Soc. Am. 53, 1608–1611.

[21] Spurr, A.R. (1969) A low-viscosity epoxy resin embedding medium for electron microscopy. J. Ultrastruct. Res. 26, 31–43.

[22] Stempack, J.C. and Ward, R.T. (1964) An improved staining method for microscopy. J. Cell Biol. 22, 697–701.

[23] Venable, H.H. and Coggeshall, R. (1965) A simplified lead citrate staining for use in electron microscopy. J. Cell Biol. 25, 407–408.

[24] Olsen, R.A. and Bakken, L.R. (1987) Viability of soil bacteria: optimization of plate-counting technique and comparison between total counts and plate counts within different size groups. Microb. Ecol. 13, 59–74.

[25] Stenstrom, J., Hansen, A. and Svensson, B. (1991) Kinetics of microbial growth- associated product formation. Swed. J. Agric. Res. 21, 55–62.

[26] Ratkowsky, D.A., Lowry, R.K., Mcmeekin, T.A., Stokes, A.N. and Chandler, R.E. (1983) Model for bacteria culture growth rate through the entire biokinetic temperature range. J. Bacteriol. 154, 1222–1226.

[27] Butler, A.R. and Walsh, D. (1982) Colorimetric nonenzymic

methods for the determination of urea. Trends Anal. Chem. 1, 120–124.
[28] Segel, I.H. (1976) Biochemical Calculations, 2nd edn., pp. 244–245. Wiley and Sons, New York.
[29] Mobarry, B.K., Wagner, M., Urbain, V., Rittmann, B.E. and Stahl, D.A. (1996) Phylogenetic probes for analyzing abundance and spatial organization of nitrifying bacteria. Appl. Environ. Microbiol. 62, 2156–2162.
[30] Stephen, J.R., McCaig, A.E., Smith, Z., Prosser, J.I. and Embley, T.M. (1996) Molecular diversity of soil and marine 16S rRNA gene sequences related to β-subgroup ammonia-oxidizing bacteria. Appl. Environ. Microbiol. 62, 4147–4154.
[31] Hankinson, T.R. and Schmidt, E.L. (1984) Examination of an acid forest soil for ammonia- and nitrite-oxidizing autotrophic bacteria. Can. J. Microbiol. 30, 1125–1132.
[32] De Boer, W., Klein Gunnewiek, P.A. and Laanbroek, H.J. (1995) Ammonium oxidation at low pH by a chemolithotrophic bacterium belonging to the genus *Nitrosospira*. Soil Biol. Biochem. 27, 127–132.
[33] Cooper, A.B. (1983) Population ecology of nitrifiers in a stream receiving geothermal inputs of ammonium. Appl. Environ. Microbiol. 45, 1170–1177.
[34] Smorczewski, W.T. and Schmidt, E.L. (1991) Numbers, activities, and diversity of autotrophic ammonia-oxidizing bacteria in a freshwater, eutrophic lake sediment. Can. J. Microbiol. 37, 828–833.
[35] Hiorns, W.D., Hastings, R.C., Head, I.M., McGarthy, A.J., Saunders, J.R., Pickup, R.W. and Hall, G.H. (1995) Amplification of 16S ribosomal RNA genes of autotrophic ammonia-oxidizing bacteria demonstrates the ubiquity of Nitrosopiras in the environment. Microbiology 141, 2793–2800.
[36] Aakra, Å., Utåker, J.B. and Nes, I.F. (1999) RFLP of rRNA genes and sequencing of the 16S-23S rDNA intergenic spacer region of ammonia-oxidizing bacteria: a phylogenetic approach. Int. J. Syst. Bacteriol. 49, 123–130.
[37] De Boer, W. and Laanbroek, H.J. (1989) Ureolytic nitrification at low pH by *Nitrosospira* spec.. Arch. Microbiol. 152, 178–181.
[38] Prosser, J.I. (1989) Autotrophic nitrification in bacteria. Adv. Microb. Physiol. 30, 125–181.
[39] Suzuki, I., Dular, V. and Kwok, S.C. (1974) Ammonia or ammonium ion as substrate for oxidation by *Nitrosomonas europaea* cells and extracts. J. Bacteriol. 120, 556–558.
[40] Knowles, G., Downing, A.L. and Barrett, M.J. (1965) Determination of kinetic constants for nitrifying bacteria in mixed culture, with the aid of an electronic computer. J. Gen. Microbiol. 38, 263–278.
[41] Stehr, G., Bötcher, B., Dittberner, P., Rath, G. and Koops, H.P. (1995) The ammonia-oxidizing nitrifying populatio of the River Elbe estuary. FEMS Microbiol. Ecol. 17, 177–186.
[42] Kohler, H.P., Heitzer, A., Hamer, G. (1991) Improved unstructured model for describing temperature dependence of bacterial maximum specific growth rates. In: Int. Symp. Environ. Biotechnol. (Verachtert, H. and Verstraete, W., Eds.), pp. 511–514. Royal Flemish Soc. Engeneers, Ostend.
[43] Diaz-Ravina, M., Frostegård, Å. and Bååth, E. (1994) Thymidine, leucine and acetate incorporation into soil bacterial assemblages at different temperatures. FEMS Microbiol. Ecol. 14, 221–223.
[44] Heitzer, A., Kohler, H.P.E., Reichert, P. and Hamer, G. (1991) Utility of phenomenological models for describing temperature dependence of bacteria growth. Appl. Environ. Microbiol. 57, 2656–2665.
[45] Anderson, O.E., Boswell, F.C. and Harrison, R.M. (1971) Variations in low temperature adaptability of nitrifiers in acid soils. Soil Sci. Soc. Am. Proc. 35, 68–71.
[46] Painter, H.A. (1986) Nitrification in the treatment of sewage and waste-waters. In: Nitrification (Prosser, J.I., Ed.), pp. 185–211. IRL Press, Oxford.
[47] Mobley, H.L.T. and Hausinger, R.P. (1989) Microbial ureases: significance, regulation, and molecular characterization. Microbiol. Rev. 53 (1), 85–108.
[48] Jeffries, C.D. (1964) Urease activity of intact and disrupted bacteria. Arch. Pathol. 77, 544–547.
[49] Jeffries, C.D. (1964) Intracellular microbial urease. Nature 202, 930.
[50] Romano, N. and LaLicata, R. (1978) Cell fractions and enzymatic activities of *Ureaplasma urealyticum*. J. Bacteriol. 136, 833–838.
[51] Jahns, T., Zobel, A., Kleiner, D. and Kaltwasser, H. (1988) Evidence for carrier-mediated, energy-dependent uptake of urea in some bacteria. Arch. Microbiol. 149, 377–383.
[52] Mclean, R.J.L., Cheng, K.-J., Lister, W.D. and Wise, R. (1986) Historchemical and biochemical urease localization in the periplasm and outer membrane of two *Proteus mirabilis* strains. Can. J. Microbiol. 32, 772–778.
[53] Booth, J.L. and Vishniac, H.S. (1987) Urease testing and yeast taxonomy. Can. J. Microbiol. 33, 396–404.
[54] Ciurli, S., Marzadori, C., Benini, S., Deiana, S. and Gessa, C. (1996) Urease from the soil bacterium *Bacillus pasteurii*: immobilization on Ca-polygalacturonate. Soil Biol. Biochem. 28 (6), 811–817.
[55] Pirt, S.J. (1975) Principles of Microbe and Cell Cultivation. Blackwell, Oxford.